IOP Conf. Series: Journal of Physics: Conf. Series **843** (2017) 012025 doi:10.1088/1742-6596/843/1/012025

Investigation of fatigue assessments accuracy for beam weldments considering material data input and FE-mode type

Yevgen Gorash*, Tugrul Comlekci and Donald MacKenzie
University of Strathclyde, MAE, James Weir Bld, 75 Montrose St, Glasgow G1 1XJ, UK
E-mail: yevgen.gorash@strath.ac.uk

Abstract. This study investigates the effects of fatigue material data and finite element types on accuracy of residual life assessments under high cycle fatigue. The bending of cross-beam connections is simulated in ANSYS Workbench for different combinations of structural member shapes made of a typical structural steel. The stress analysis of weldments with specific dimensions and loading applied is implemented using solid and shell elements. The stress results are transferred to the fatigue code nCode DesignLife for the residual life prediction. Considering the effects of mean stress using FKM approach, bending and thickness according to BS 7608:2014, fatigue life is predicted using the Volvo method and stress integration rules from ASME Boiler & Pressure Vessel Code. Three different pairs of S-N curves are considered in this work including generic seam weld curves and curves for the equivalent Japanese steel JIS G3106-SM490B. The S-N curve parameters for the steel are identified using the experimental data available from NIMS fatigue data sheets employing least square method and considering thickness and mean stress corrections. The numerical predictions are compared to the available experimental results indicating the most preferable fatigue data input, range of applicability and FE-model formulation to achieve the best accuracy.

1. Introduction

Connection by welding is the most effective fabrication process, which is used for a relatively fast manufacturing of big assemblies using simple structural members. Welded joints between metal parts are produced by causing fusion, which includes melting the the base metal and adding the filler material. The phase transformation of even a small amount of the structural material usually results in significant residual stresses, heat effected zone with weaker mechanical characteristics, rugged surface geometrical features and various welding defects – cracks, distortion, inclusions, incomplete penetration, etc. – refer to [1] for more details. In general, the nature of the welding process means that weldments have a lower fatigue strength than the base material of the parts, which are joined together. The negative effect of welding on the integral strength of the structure is usually minimised during the design process. For example, welded joints need to be kept away from highly stressed areas, since they increase the stresses even more. An infinite fatigue life can be theoretically provided for the base material by identification of the fatigue strength limit, which can be used as a stress limit in the design analysis. Thus, by a proper positioning of weldments the main loading can be carried out primarily by the base material providing an infinite fatigue life. However, even in well-designed

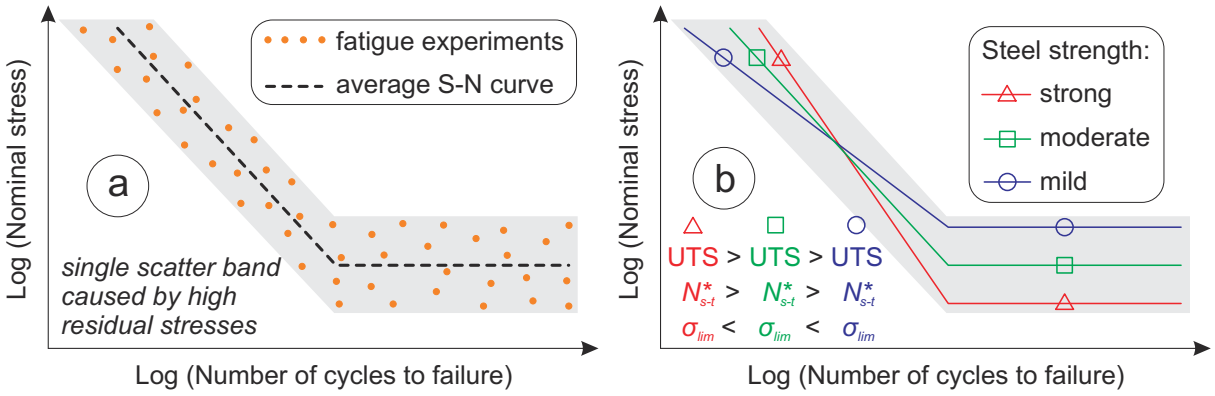

Figure 1. Fatigue strength of weldments in relation to the strength of base metal: a) conventional approach to S-N curve, b) investigated observations.

structures, where the weldments are placed away from the load path, the fatigue failures are typically found in weldments [2]. Therefore, the residual life prediction for welded structure should be based in the first instance upon fatigue analysis of weldments [1].

The fatigue behaviour of weldments has been studied in terms of the geometry of the members, the stresses to which they are subjected, and the materials of which they are fabricated [3]. In regard to the choice of base material, there are a few experimental observations, which may explain its relation to the fatigue strength of corresponding weldments. Within the conventional approach, when steels of widely differing grades are welded, the resulting S-N curves tend to fall within a single scatter band, as shown in Fig. 1a. The principal reason for this is that superior fatigue strength of high-strength steels as base material is eliminated by the high residual stresses in the welds, which usually approaches the yield strength. However, closer examination of the fatigue curve slopes reveals that low-strength steels (with lower σ_u) tend to have better fatigue resistance in long-term domain under low loads while high-strength steels (with higher σ_u) tend to have better fatigue strength in short-term domain (N^*_{s-t}) under high loads, as shown in Fig. 1b. The detailed discussion of this observation is available in [4, 5], which conclude that the fatigue strength of weldments is not completely independent of the base material strength, it is rather inversely proportional to the σ_u of the base material. Therefore, provision of more specific S-N curves for different groups of steels (e.g. mild, moderate and hard) may increase the quality of fatigue assessments. This paper addresses the comparison of specific S-N curve and generic S-N curves for investigation of accuracy of residual life predictions for welded structures.

The most effective way of fatigue assessment is a postprocessing of FEA results of a structural analysis in the form of stress / strain fields (geometry input) in combination with input of load history and fatigue material data. There is a variety of fatigue assessment tools available for FEA from basic tools in form of add-ins or modules for CAD/CAE products to advanced stand-alone or integrated fatigue postprocessors [6]. The fatigue code nCode DesignLife embedded in ANSYS Workbench environment has been chosen for this study, since a number of advanced features have been implemented in it to facilitate the effective fatigue analysis of welds. The main methods implemented in nCode DesignLife with theoretical background on fatigue of welds and validation cases are outlined in [2, 7].

It should be noted that in total majority of published studies the specific modules for weld fatigue analysis were not used, the investigators preferred conventional approaches like hot-spot stress or notch stress methods which required structural stress from FEA as input. In contrast to previous works, this study investigates the robustness of the available seam weld fatigue analysis module of nCode DesignLife which is based on nominal stress method in application

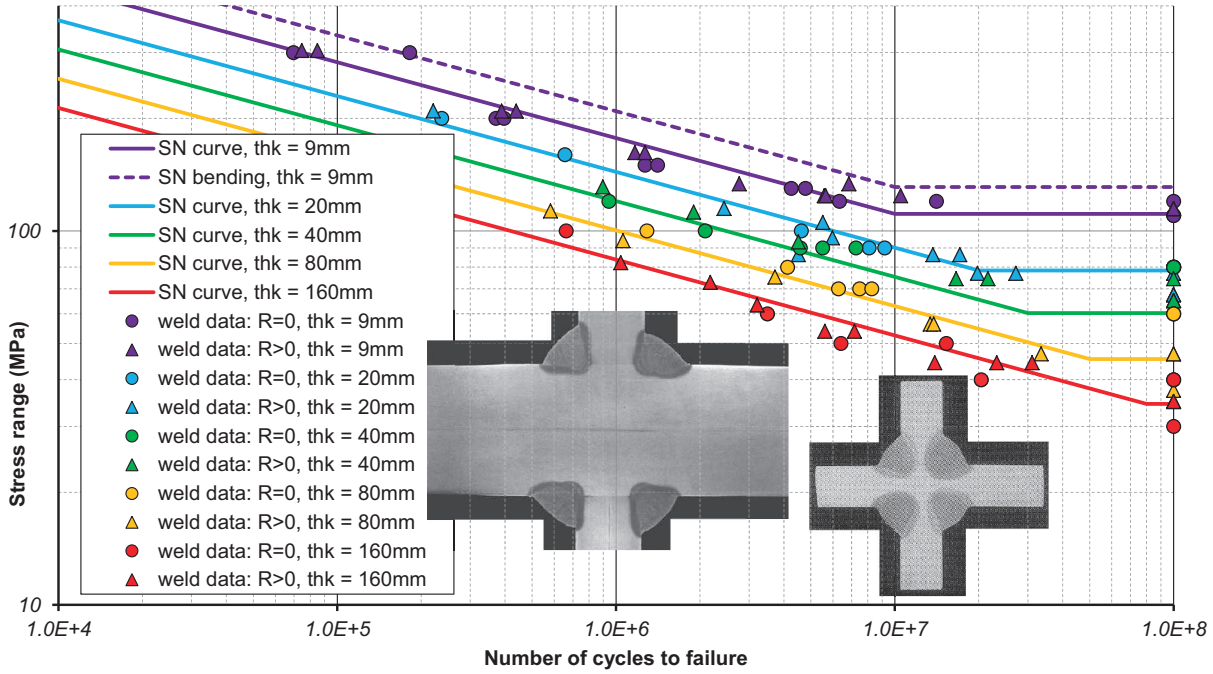

Figure 2. Experimental and fitted S-N curves of cruciform welded joints made of SM490B steel for different thicknesses [10] and normalised to $R = 0$.

to solid and shell FE-models. This paper presents a numerical comparative study in order to validate not only available analysis facilities in nCode DesignLife for weld models in solid and shell formulation, but also the significance of fatigue material data input. This work is built on the outcomes of the initial study [4] and develops it further considering a proper induction of the mean stress correction and finalising the fatigue assessments for solid FE-models of all weldment configurations. The experimental studies of welded thin-walled cross-beam connections under cyclic bending by Mashiri *et al.* [8, 9] have been chosen as a validation in this numerical study.

2. Handling the fatigue properties of weldments

The specimens in experiments [8, 9] were manufactured from cold-formed high-strength steel of grades C350LO (σ_y = 350 MPa and σ_u = 430 MPa) and C450LO (σ_y = 450 MPa and σ_u = 500 MPa) according to the Australian Standard AS3678. These two grades represent the lower (Grade C350) and upper (Grade C450) bounds of the big international group of weldable, general-purpose, high-strength structural steels, which includes the following grades [11]: *Grade 50 (A, B, C, D)* from British Standard BS4360; *St52-3* from German Standard DIN17100; *G3106-SM490 (A, B, C)* from Japanese Standard JIS; *Fe510 (B, C, D)* from International Standard ISO630; *A572-345 (-415)* from American Standard ASTM; *S355 (JR, J0, etc.)* from European Standard EN10025.

These steels are roughly equivalent in chemical composition and have similar elastic properties with elastic modulus of $E = 2 \cdot 10^5$ MPa and Poisson's ratio of $\nu = 0.3$. Since specific fatigue curves for the weldments made of grades C350 or C450 are unavailable in the nCode DesignLife material database, an equivalent fatigue data input is required. The principal aspect in fatigue of weldments is availability of the appropriate experimental data for a long-term strength domain. The most suitable fatigue datasets of this kind are provided by National Institute for Materials Science (Tsukuba, Japan) for the Japanese equivalent from the list above – steel SM490B. The datasets are presented by 5 NIMS Fatigue Data Sheets [10] available in 5 parts for cruciform

Table 1. Fatigue constants for three variants of the material, different types of amplitude, values of stress ratio R and reference thickness t_{ref}.

material	No.	amplitude	t_{ref} [mm]	n	R	*bending*	*SRI* [MPa]	b	slope *(1/b)*
SM490B steel welds	1a	CA	9	0.26	0	stiff	2914.8	0.2027	4.93
						flex	3439.5	0.2027	4.93
	1b	CA	1		0	stiff	5160.7	0.2027	4.93
						flex	6089.7	0.2027	4.93
generic SN curves from nCode DL	2a	VA	1	0.16667	-1	stiff	18000	0.3333	3.00
						flex	36000	0.3333	3.00
	2b	CA	1		-1	stiff	25960	0.3333	3.00
						flex	51920	0.3333	3.00
	2c	CA	1		0	stiff	20768	0.3333	3.00
						flex	41536	0.3333	3.00
generic SN curves from nCode FEF	3a	VA	3	0.16667	-1	stiff	8569	0.2632	3.80
						flex	11478	0.219	4.57
	3b	CA	3		-1	stiff	13090	0.2632	3.80
						flex	17534	0.219	4.57
	3c	CA	1		-1	stiff	13090	0.2632	3.80
						flex	17534	0.219	4.57
	3d	CA	1		0	stiff	10472	0.2632	3.80
						flex	14027	0.219	4.57

weldments of 5 different thicknesses (9 mm, 20 mm, 40 mm, 80 mm, 160 mm), which provide the details of fatigue tests with stress ratio R from 0 to 1 and duration of experiments up to 10^8 cycles, as illustrated in Fig. 2. This experimental data needs to be properly fitted by an S-N curve equation, which is adapted to fatigue analysis capabilities implemented in nCode DesignLife, and corresponding fatigue parameters need to be accurately identified.

An advantage of nCode DesignLife as a fatigue postprocessor in the availability of effective approaches for fatigue analysis of weldments in both shell and solid elements formulations. The important feature of these approaches is that they are relatively non-sensitive to the quality of finite element mesh. The "Volvo" Method [12], used for coarse shell models, is suitable for making FE-based fatigue assessments of welded joints with the minimum of user intervention being required [2, 7]. Weld fatigue analysis in application to the solids requires more efforts compared to shells as discussed in [5, 2, 7]. The key element of this approach is the stress integration method proposed in ASME BPVC Code [13], when the stress is extracted at several points through thickness, and then extrapolated to produce membrane and bending components. Recently the fatigue analysis in solid formulation has been drastically improved and accelerated with the release of an ACT extension for ANSYS Workbench titled nCode Weldline [14], which brings a dramatic progress into the analysis of complex assemblies with a free-form geometry and arbitrary location of welded joints [5].

An essential feature of fatigue analysis is the mean stress effect, which needs to be carefully considered in this work. Weld fatigue assessment is based on a mean stress correction using the FKM approach [15], in which the mean stress sensitivity is defined by 4 factors in 4 regimes: $R > 1$, $-\infty \leq R < 0$, $0 \leq R < 0.5$, $0.5 \leq R < 1$. The idea of FKM method is usually illustrated in the form of a constant life or Haigh diagram, where the factors M_{1-4} correspond to the slopes in coordinates of mean stress σ_{m} and stress amplitude σ_{a}. In contrast to classical mean stress correction approaches (like Goodman, Gerber or Soderberg), the FKM approach is not related to material characteristics σ_{y} and σ_{u}. It also allows to determine the equivalent stress amplitude σ_{a} at a particular material R-ratio, but it has better applicability for characterisation of environmental (corrosion / erosion) and technological (welding) effects on fatigue life. In

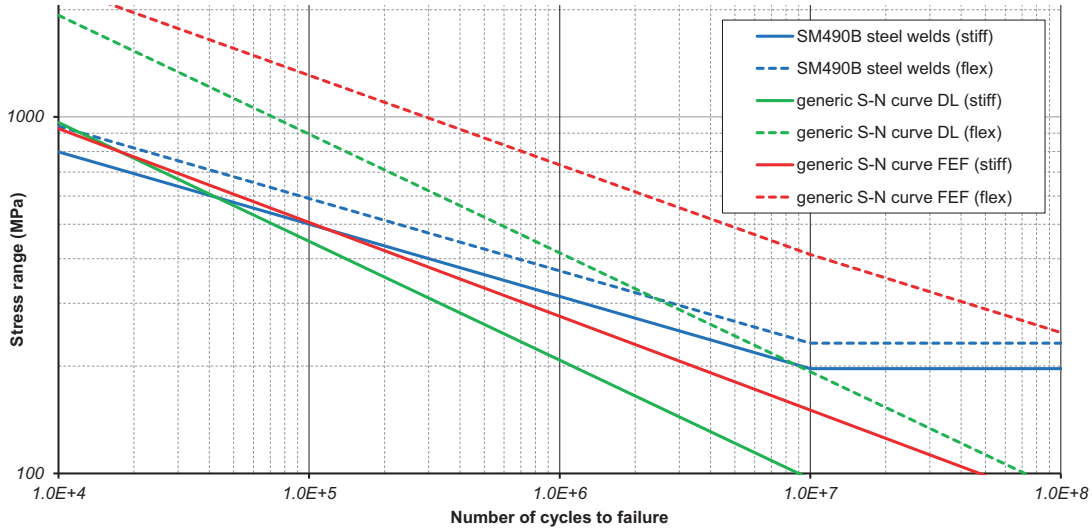

Figure 3. Comparison of three pairs of S-N curves to be used in weldments fatigue analysis, which are normalised to $t_{\mathrm{ref}} = 1$ mm of and $R = 0$.

definition of the generic S-N curves used for fatigue analysis of weldments, the nCode guidelines [2, 7] recommend the following values of the FKM factors: $M_1 = 0$, M_2 = -0.25 and $M_3 = M_4$ = -0.1. For the specific steel SM490B, these factors may have different values and need to be identified using the available experiments [10] in the range $0 < R < 1$.

Other important effects directly related to the fatigue of welds are bending and thickness effects, which are included in fatigue analysis according to the British Standard BS7608 [16]. If a reference thickness is exceeded, the fatigue strength is reduced by a correction factor:

$$k_{\mathrm{tb}} = \left(\frac{t_{\mathrm{ref}}}{t}\right)^{n} \left[1 + 0.18\,\Omega^{1.4}\right], \tag{1}$$

where t – thickness of the welded components, t_{ref} – reference thickness, n – thickness exponent.

In notation (1), the fatigue strength increases with increasing bending component (defined by bending ratio Ω) for a decreasing stress range gradient through the thickness. However, the design S-N curves relate to applied loading conditions that produce predominantly membrane stresses. So the S-N curve corresponding to pure bending condition can be obtained from a basic membrane S-N curve by setting the bending ratio $\Omega = 1$. The potentially detrimental effect of increased thickness but beneficial effect from applied bending are combined by the application of the correction factor k_{tb} using Eq. (1) to the stress ranges $\Delta\sigma_{\mathrm{b}}$ obtained from the relevant basic S-N curve [16]:

$$\Delta\sigma = k_{\mathrm{tb}}\,\Delta\sigma_{\mathrm{b}}, \tag{2}$$

where $\Delta\sigma$ is a nominal stress range in the structural component under consideration of bending and thickness correction. The basic S-N curve is fitted using the standard nCode DesignLife definition, where the curve consists of 3 linear segments on a log-log plot. The central and long-term domains are defined by the formula [7]:

$$\Delta\sigma_{\mathrm{b}} = \begin{cases} I_{\Delta\sigma 1}\, N_*^{-b_1} & \text{if} \quad N_* < N_{C1} \\ I_{\Delta\sigma 1}\, N_{C1}^{(b_2-b_1)}\, N_*^{-b_2} & \text{otherwise} \end{cases}, \tag{3}$$

where N_* – number of cycles to failure; $I_{\Delta\sigma 1}$ – stress range intercept (MPa); b_1 – first fatigue strength exponent; N_{C1} – transition life; b_2 – second fatigue strength exponent. Transition life

N_{C1} defines the point on the curve, where it transitions to the second slope b_2. If b_2 is set to zero, this acts as a fatigue limit.

For the purpose of accurate identification of fatigue parameters, the original set of experimental data [10] for steel SM490B welds available for the range of thicknesses t and stress ratios R needs to be normalised to the equality condition with $t_{\rm ref} = 9$ mm and $R = 0$. The R-normalisation of the stress range $\Delta\sigma_{\rm R0} = 2\,\sigma_{\rm a0}$ is obtained using the idea of FKM mean stress correction as explained in [5]. The t-normalisation of the stress range $\Delta\sigma_{\rm t9}$ is done using the thickness correction in form (1) as

$$\Delta\sigma_{\rm t9} = \Delta\sigma \ (t_{\rm ref} \ / \ t)^{-n} \,, \tag{4}$$

where the thickness exponent n is unknown.

The resultant set of experimental data [10] after normalisation is fitted with Eq. (3) as illustrated in Fig. 4. The fitting accuracy is characterised by the coefficient of determination R^2, which needs to be maximised for the best result. A manual optimisation procedure based on enumeration with the goal to maximise R^2 and determine corresponding values of M_3 and n was implemented in MS Excel. Using the step of 0.0001 for M_3 in the range from 0.015 to 0.03 and the step of 0.001 for n in the range from 0.2 to 0.3 the global maximum value of $R^2 = 0.9484959$ has been achieved with corresponding values of $M_3 = -0.0283$ and $n = 0.26$. The least squares fit of the power function to the normalised experimental data as shown in Fig. 4 results into the constants set No. 1a for constant amplitude (CA), which is listed in Table 1 with additional constants for long-term domain as $b_2 = 0$ and $N_{C1} = 10^7$, as recommended in BS7608 [16]. This constants set for steel SM490B welds is complemented by the remaining FKM factors as recommended in [15]: $M_1 = 0$, $M_2 = 3 \cdot M_3$ = -0.0849 and $M_4 = M_3$ = -0.0283.

The result of fitting with Eq. (3) is illustrated in Fig. 2 with solid blue line. The result of bending correction for $\Omega = 1$ using Eqs (1) and (2) is shown with the dashed blue line. The result of thickness correction using Eqs (1) and (2) is shown with solid lines for thicknesses 20, 40, 80, 160 mm. Since $t_{\rm ref} = 9$ mm for the constants set No. 1a, it produces very conservative fatigue life predictions for the welded components with $t < 9$ mm. Thus, the constants need to be extrapolated up to $t_{\rm ref} = 1$ mm to become suitable for fatigue analysis of structural members used in experiments by Mashiri *et al.* [8, 9] having thicknesses as $t = 1.4$ mm, 3 mm and 4 mm. This transformation is done combining Eqs (1)-(3) as

$$I^{t}_{\Delta\sigma 1} = I_{\Delta\sigma 1}\,(t_{\rm ref} \ / \ t^{new}_{\rm ref})^{n} \,, \tag{5}$$

where $t^{new}_{\rm ref}$ is a new reference thickness and $I^{t}_{\Delta\sigma 1}$ is a new corresponding stress range intercept. Using the value of $t^{\rm new}_{\rm ref} = 1$ mm in Eq. (5), the constant set No. 1a is transformed into the constant set No. 1b, which is listed in Table 1 and illustrated in Fig. 3 with solid and dashed blue S-N curves. This constants set is used in nCode DesignLife for the fatigue analysis of weldments as a specific user fatigue data input characterising the material of weldments.

The advantage of specific fatigue data input needs to be confirmed by comparing it to the generic S-N curves for seam welds made of weldable structural steels available in nCode software databases. DesignLife material database contains a pair of generic S-N curves with the standard slope $1/b = 3$, $t_{\rm ref} = 1$ mm and constants given in Table 1 under No. 2a for the assumption of variable amplitude (VA). This assumptions means that $N^{CA}_{*} = 3\ N^{VA}_{*}$, because the quality of production is not as good as specimens resulting into Miner's sum effectively reducing to 1/3. Mathematically transformation from VA to CA is expressed by increase of the stress range intercept as

$$I^{CA}_{\Delta\sigma 1} = I^{VA}_{\Delta\sigma 1}\,(1/3)^{-b_1} \,, \tag{6}$$

where $I^{CA}_{\Delta\sigma 1}$ and $I^{VA}_{\Delta\sigma 1}$ are the stress range intercepts for CA and VA correspondingly. Using Eq. (6), the constant set No. 2a for VA is transformed into the constant set No. 2b for CA,

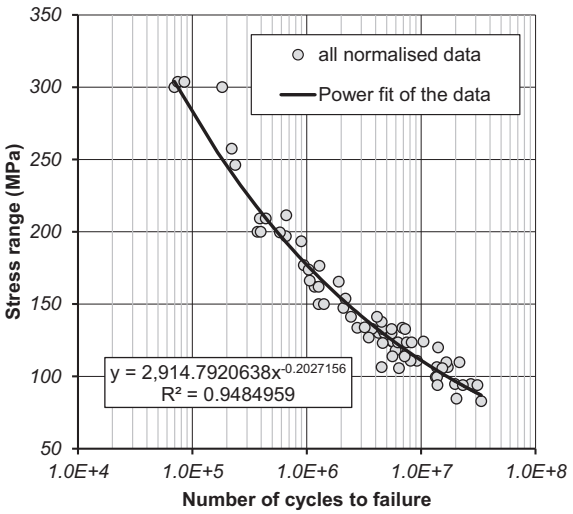

Figure 4. All fatigue data from [10] normalised to $t_{\text{ref}} = 9$ mm and $R = 0$.

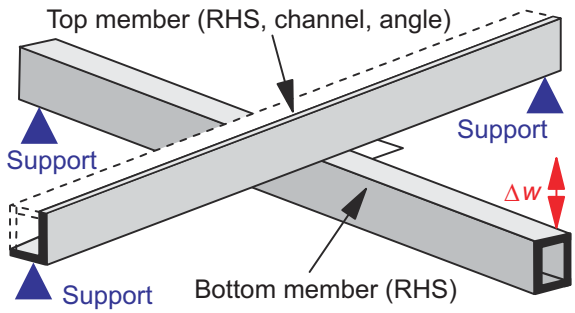

Figure 5. The fatigue tests for RHS / Channel / Angle to RHS welded cross-beam connections [8, 9] are addressed for simulations in current study.

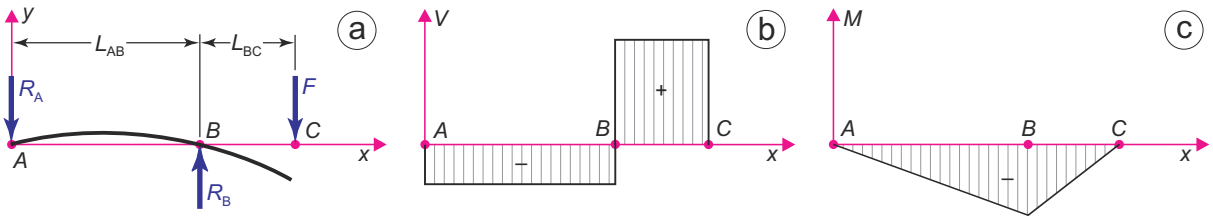

Figure 6. Diagrams of (a) vertical deflection Y, (b) shear force V, (c) bending moment M for overhanging load applied to simply supported beam [17].

which is listed in Table 1. This constants set is used in nCode DesignLife for the fatigue analysis of weldments as a recent formulation of generic fatigue data input, which has been revised to meet the requirement for standard S-N curve slope of 3.

An alternative and older generic fatigue data input considered in this works is a pair of generic S-N curves for seam welds with slopes different from standard (3.8 and 4.57) from nCode FE-Fatigue, a legacy fatigue postprocessor from nCode, predecessor of DesignLife. These S-N curves are described by the constants set No. 3a for $t_{\text{ref}} = 3$ mm and VA, which is given in Table 1 and historically preceded the set No. 2a. In order to be compared to the sets No. 1b and 2b, this constants set No. 3a requires a transformation. Firstly, Eq. (6) is used to do a VA-CA transformation resulting into the set No. 3b. Secondly, Eq. (5) is used to do reduce t_{ref} from 3 mm to 1 mm resulting into the set No. 3c listed in Table 1.

For a proper graphical comparison, all three sets of fatigue constants should correspond to the same stress ratio R, e.g. 0 as in case of the set No. 1b. Hence the sets No. 2b and 3c need to be converted from $R = -1$ to $R = 0$ using FKM mean stress correction as explained in [5]. The obtained sets No. 2c and 3d are shown in Fig. 3 with green and red S-N curves correspondingly and compared to the set No. 1b (blue curves). The visual comparison clearly indicates that the nCode DL set (2c) is going to provide the most conservative fatigue life predictions with the nCode FEF set (3d) giving non-conservative predictions, while the SM490B set (1b) will be somewhere in between nCode DL and FEF outputs with moderate fatigue life predictions.

Table 2. Dimensions of 6 variants of the beam cross-sections [mm] according to [18, 19] and corresponding area moments of inertia [mm^4].

Square Hollow Sections				Rectangular Hollow Sections	
50x50x3 SHS	50x50x1.6 SHS	35x35x3 SHS	35x35x1.6 SHS	50x25x3 RHS	50x25x1.6 RHS
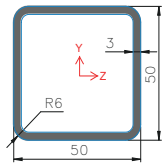	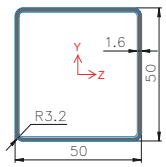	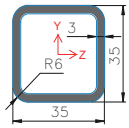	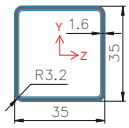	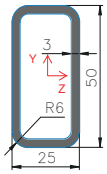	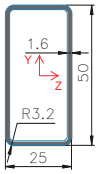
194671.36	117050.41	59483.1	37886.23	111721.36	70182.15

3. FEA-based fatigue assessment of weldments

The specimens in experiments [8, 9] had three ends (left bottom and two top supports) constrained to ground using the hinge coupling and one end left free, as illustrated in Fig. 5. This unconstrained right bottom support has an out-of-plane orthogonal displacement w applied cyclicly, which corresponds to a particular nominal stress range $\Delta\sigma$. The values of $\Delta\sigma$ for each experiment having particular cross-beam connection are reported in [4, 5]. Using the stress ratio $R = 0.1$ from the fatigue experiments [8, 9], the nominal stress range $\Delta\sigma$ can be converted into the maximum nominal stress $\sigma_{\max}$ using the following equation:

$$\sigma_{\max} = \sigma_{\text{ave}} + \sigma_{\text{a}}, \tag{7}$$

with

$$\sigma_{\text{ave}} = \sigma_{\text{a}} \frac{1+R}{1-R} \quad \text{and} \quad \sigma_{\text{a}} = \frac{\Delta\sigma}{2}, \tag{8}$$

where σ_{ave} is an average nominal stress and σ_{a} is a nominal stress amplitude. The values of $\sigma_{\max}$ reported in [4, 5] are required for the assessment of corresponding out-of-plane displacement w applied to the unconstrained beam end.

For the assessment of w, the case of overhanging load applied to simply supported beam available from [17] and shown in Fig. 6, is used as a structural equivalent to the cross-beam connection. In this case, locations A and B on a beam from the simplified model are vertically constrained, and the location C has the orthogonal force applied to it. In experiments [8, 9], location A corresponds to the left constrained end of the bottom beam, location B – toe of the weld connecting the beams, and location C – right unconstrained end of the bottom beam. The analytical solution for a structural analysis problem with overhanging load applied to a simply supported beam is provided in [17] including equations and diagrams for vertical deflection Y, shear force V and bending moment M, which are shown in Fig. 6. The most relevant for this study is the equation for deflection of the beam in location C, which is further used as w:

$$Y_{\text{C}} = -\frac{F\, L_{\text{BC}}^2\, (L_{\text{AB}} + L_{\text{BC}})}{3\, E\, I_{\text{Z}}}, \tag{9}$$

where E is an elastic modulus for the material of beam taken from Sec. 2, and I_{Z} is an area moments of inertia [mm^4] about the neutral axis Z for the beam cross-section. The particular values of I_{Z} for six variants of the beam profiles for the bottom member are reported in Table 2. These values are calculated using the real geometry of beam profiles in CAD-software SolidWorks with dimensions from Australian / New Zealand standard [18] and technical specification [19], which are shown in Table 2. The beam profile is considered to be located in $Y - Z$ plane with

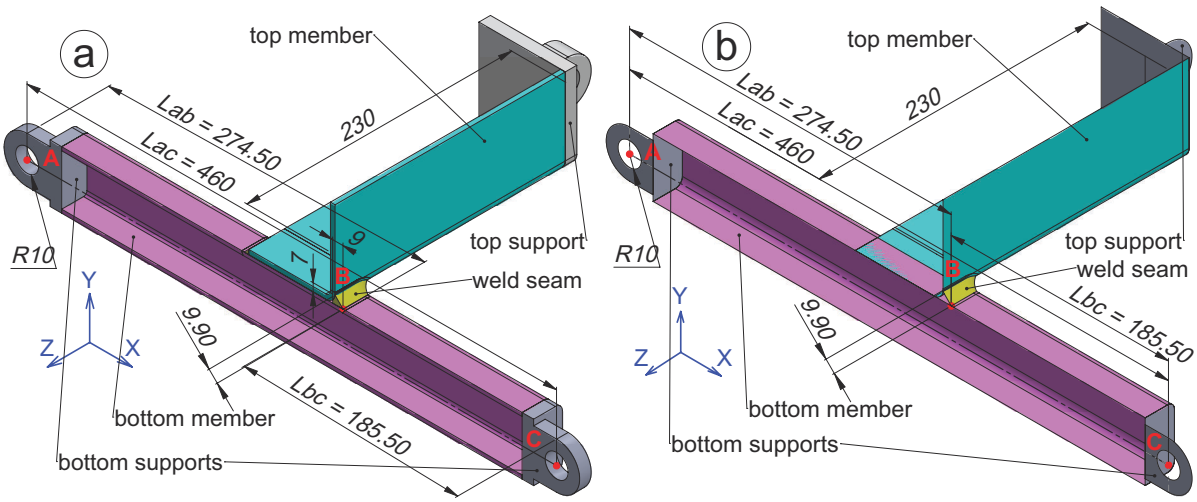

Figure 7. Geometry, components definition and dimensions (mm) for 75x75x4 CA to 50x50x3 SHS connection using (a) solids and (b) surfaces.

the neutral axis Z going through the profile centre. Therefore, a beam representing the bottom member bends around the axis Z. In notation (9), the applied bending force F is estimated using the assumption of maximum bending stress being the maximum nominal stress $\sigma_{\max}$ in experiments. Referring to the design guide [20], in experiments [8, 9] the nominal stress is caused by the basic load, which was the "bending moment in the bottom member". So the bending force F is obtained from the classic formula for determining the maximum bending stress in the outermost layer of the beam under simple bending as:

$$\sigma_{\max} = \frac{M\,H_{\mathrm{Y}}}{I_{\mathrm{Z}}} = \frac{F\,L_{\mathrm{BC}}\,H_{\mathrm{Y}}}{I_{\mathrm{Z}}} \quad \Longrightarrow \quad F = \frac{\sigma_{\max}\,I_{\mathrm{Z}}}{L_{\mathrm{BC}}\,H_{\mathrm{Y}}}, \tag{10}$$

where M is the moment about the neutral axis Z and H_{Y} is the perpendicular distance from the outermost layer of the beam to the neutral axis Z, which in this case corresponds to the half height of the section profile indicated in Table 2.

Equations (9) and (10) are used to estimate the values of w corresponding to $\sigma_{\max}$ with additional input of parameters specific for each experiment like I_{Z}, L_{AB} and L_{BC}. The resultant values of the displacement w, which is applied to the right end of bottom member as illustrated in Fig. 5, are reported in [4, 5].

The comprehensive geometrical models of welded cross-beam connections were created in CAD-software SolidWorks in solids and surfaces presentation including top and bottom members, top and bottom supports, and the weld seam. The dimensions of beam profiles are taken from Australian / New Zealand standard [18] and technical specification [19]. All variants of tubes (RHS/SHS), angles (CA) and channels (CC) are listed in detailed reports [4, 5]. It should be noted that the specimens geometry can be simplified to a half model (not a quarter) using the vertical symmetry plane along the bottom member (except channel-to-channel connection which requires full model), because of the unsymmetric loading and deformation. The example of the geometry for the connection of 75x75x4 CA (top member) to 50x50x3 SHS (bottom member) is shown in Fig. 7a using solids and in Fig. 7b using surfaces. The distance between centres of supports in this work is assumed to be 460 mm. In accordance to the 2D model of a simply supported beam in Fig. 6, the points A, B and C are denoted in Fig. 7. The legs of welds around the rounded corners are 9 mm (horizontal) and 7 mm (vertical) giving 8 mm in average in compliance with experiments [9]. The weld face length is 9.9 mm, and the weld throat

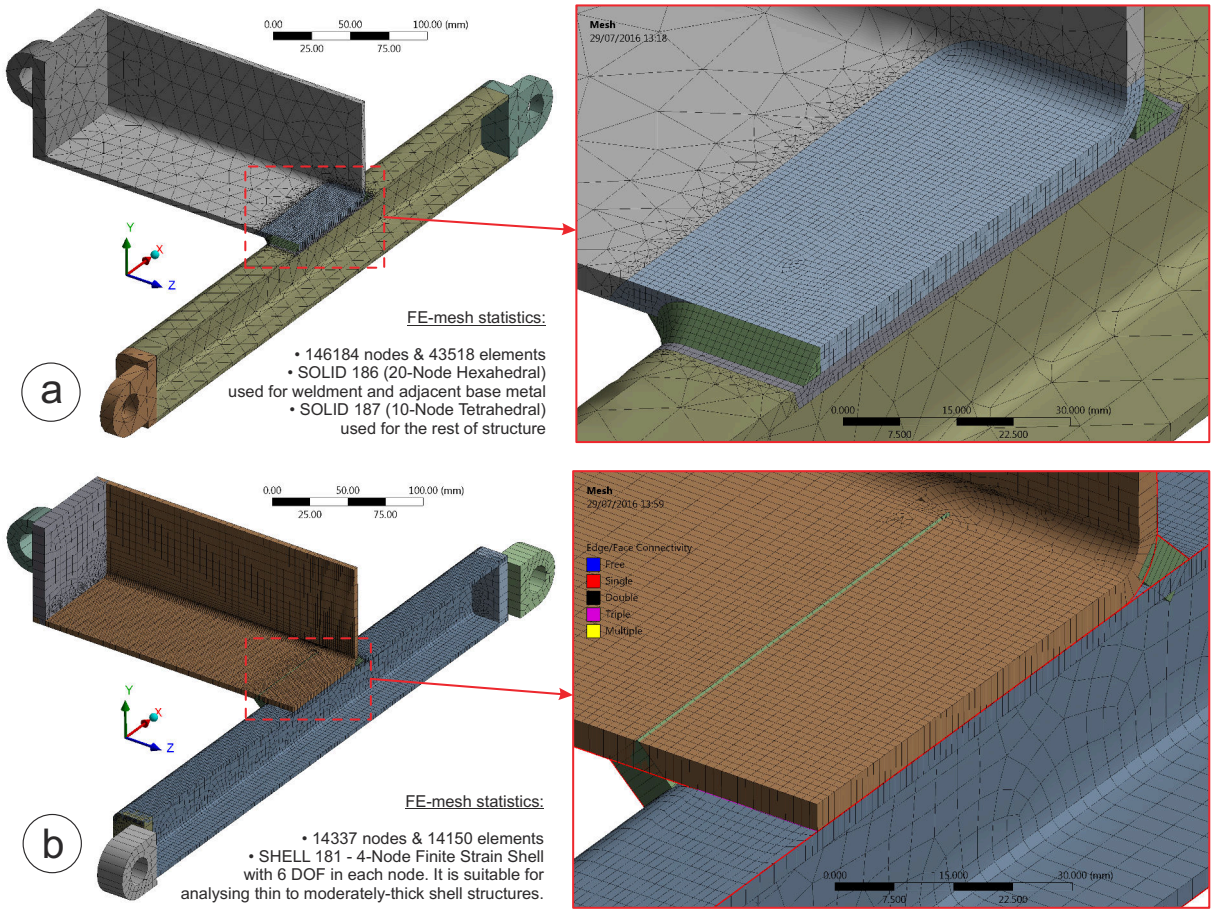

Figure 8. FE-mesh, statistics and blowup of the weldment area for 75x75x4 CA to 50x50x3 SHS connection using (a) solid FEs and (b) shell FEs.

considered in shell model formulation is 6 mm. The example of the FE-mesh corresponding to the configuration 75x75x4 CA to 50x50x3 SHS, together with mesh statistics and blowup of the location of contact between the beams are shown in Fig. 8a using solid FEs and Fig. 8b using shell FEs. It should be noted that the solution of the shell model is performed much quicker than the solution of the solid model since the number of solved equations expressed in the number of nodes is 10 times smaller for the shell model.

In solid model setup, the hinge type of constraint is applied to 3 constrained supports (points A and B in Fig. 7) as illustrated in Fig. 5, which assumes only 1 rotational degree of freedom (DOF) around the longitudinal axis and excludes any translation along the same axis. In shell model, the same boundary condition (BC) applied to same 3 supports is carried out by constraining: {1} 2 in-plain displacements (equivalent to constraining the radial displacement), {2} 2 out-of-plain rotations (which are constrained in cylindrical coupling automatically) and {3} axial translation in horizontal direction. This results in single rotational DOF in each of 3 supports and the vertical displacement applied to the centre of 4th support directed downwards. It should be noted that compared to previous study [4], where the cylindrical type of constraint (1 rotational DOF + 1 translational DOF) was applied to 3 constrained supports, this study uses the hinge type of constraint to agree more accurately with experimental setup [8, 9]. This modification of BCs results in slight increase of equivalent von Mises stress up to 10% and corresponding decrease in predicted fatigue life using shell FE-models when compared to the

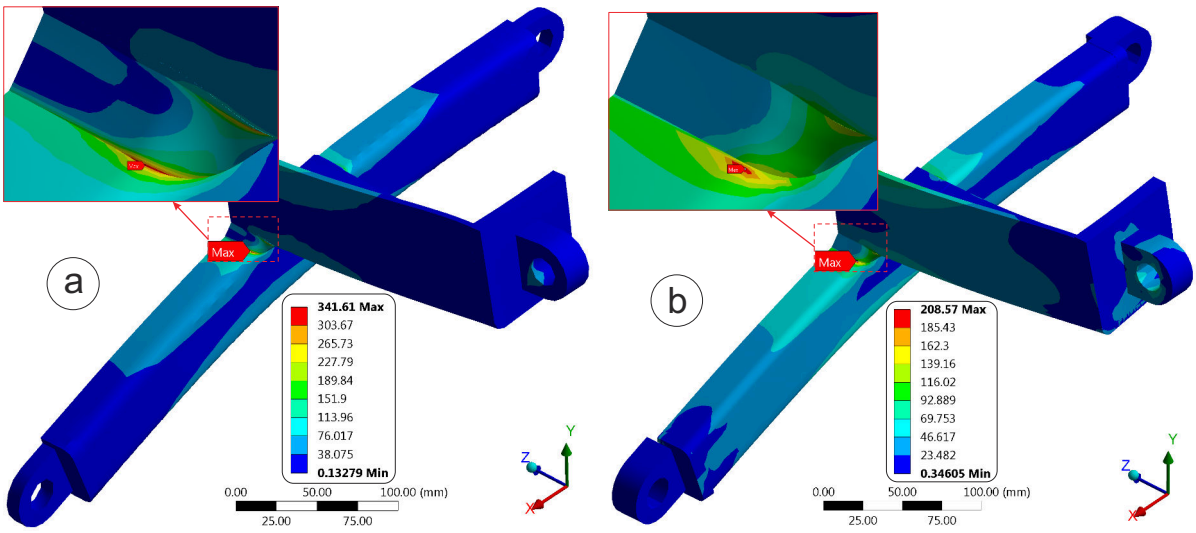

Figure 9. Equivalent von Mises stress (MPa) for 75x75x4 CA to 50x50x3 SHS connection for (a) solid FE-model and (b) shell FE-model.

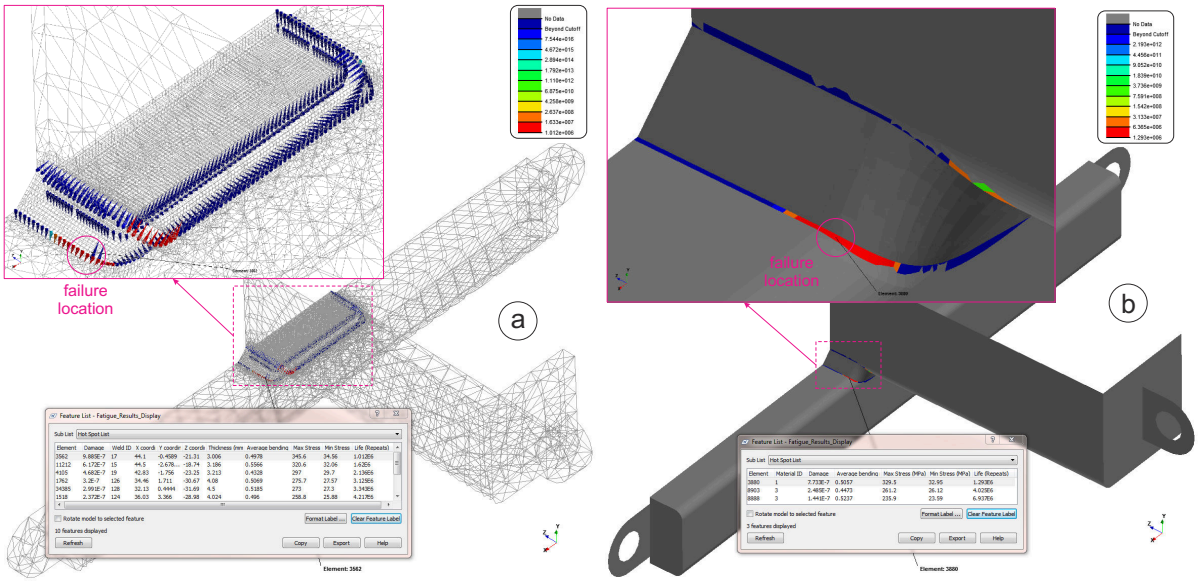

Figure 10. Result of fatigue life predictions (cycles) for 75x75x4 CA to 50x50x3 SHS connection for (a) solid FE-model and (b) shell FE-model.

results reported in previous study [4].

With equivalent BCs and loads applied to FE-models, the maximum values of equivalent von Mises stress obtained in result of structural analyses in solid models are up to two times bigger than in shell models. The examples of stress distribution together with blowup of the area of the highest stress are shown in Fig. 9a using solid FEs and in Fig. 9b using shell FEs for 75x75x4 CA to 50x50x3 SHS connection. Such a difference in maximum stress values is explained by the assumption that shell FE-model output a maximum hotspot stress in vicinity of the weld toe, while the maximum stress in solid FE-model is observed exactly on the sharp edge and mostly contributed by a non-linear component of structural stress caused by geometrical singularity.

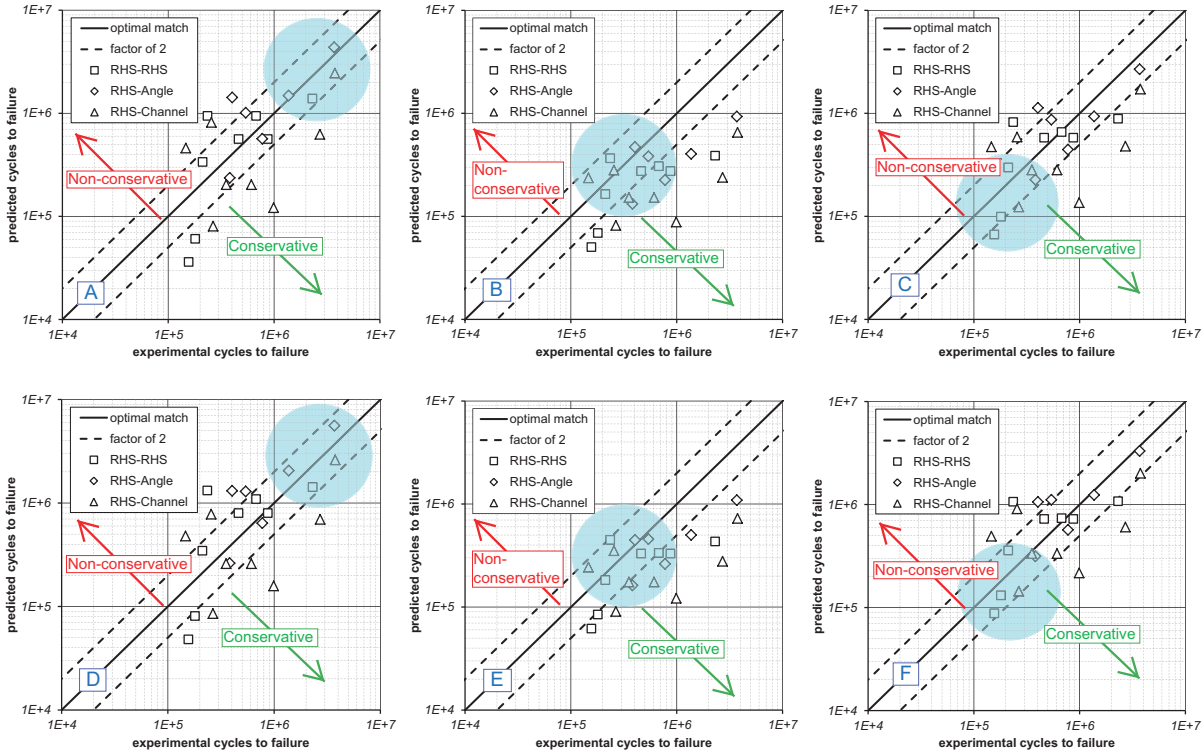

Figure 11. Comparison of the observed and predicted cycles to failure using solid (top) and shell (bottom) FE-models for: (A & D) S-N curves for SM490B steel welds {1}; (B & E) new generic S-N curves in nCode DesignLife {2}; (C & F) old generic S-N curves in nCode FE-Fatigue{3}.

4. Discussion

The results of fatigue life predictions are obtained for solid and shell formulation for 3 variants of cross-beam connections: {1} tube [RHS] to tube [RHS/SHS], {2} angle [CA] to tube [RHS/SHS], and {3} channel [CC] to tube [RHS/SHS]. Three variants of fatigue data input for CA and $t_{\text{ref}} = 1$ mm from Table 1 are used in predictions: {1} S-N curves of SM490B steel welds (set no. 1b), and generic S-N curves from {2} nCode DesignLife (set no. 2b) and {3} nCode FE-Fatigue (set no. 3c). The examples of fatigue life predictions for the connection of 75x75x4 CA to 50x50x3 SHS beams using S-N curves {1} together with blowup of the crack location are shown in Fig. 10a using solid FEs and in Fig. 10b using shell FEs. The advantage of all performed numerical predictions is that the crack has been predicted exactly in the same location as in experiments [8, 9] – front part of the weld toe on the fillet of the bottom member. The numerical predictions N_*^{FE} are compared to the experimental fatigue life N_*^{exp} numerically [4, 5] and graphically in Fig 11 (top) for solid FE-models and Fig 11 (bottom) for shell FE-models using the following formula for discrepancy in percents %:

$$\Delta N_* = \frac{100\ (N_*^{exp} - N_*^{FE})}{\min(N_*^{exp}, N_*^{FE})}. \tag{11}$$

This value characterises not only the relative deviation, but also the amount of conservatism, which is defined by the sign of this value: positive – conservative and negative – non-conservative. The total value of discrepancies are calculated for three groups of experiments (RHS-RHS/SHS, CA-RHS/SHS, CC-RHS/SHS) – these and aggregate values for all considered experiments are reported in [4, 5].

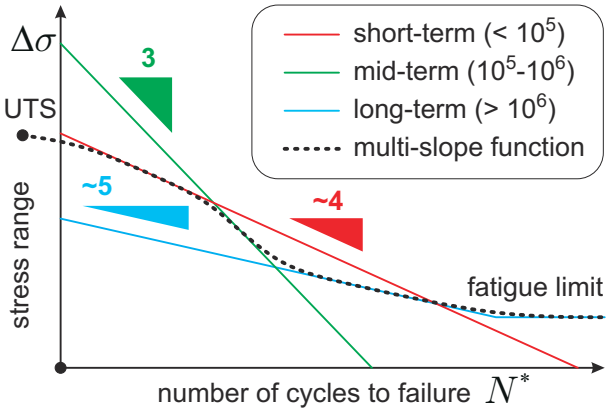

Figure 12. Multiple slopes of S-N curves are used for the formulation of a continuous function for the integral S-N curve covering all fatigue ranges.

The fatigue predictions for channel-to-tube group are the most conservative, for corner-to-tube group are less conservative, and for tube-to-tube group are non-conservative. When comparing the S-N curves input, it is clear from Figs 11b and 11e that the S-N curves {2} produce over-conservative predictions. The predictions using S-N curves {1} in Figs 11a and 11d and S-N curves {3} in Figs 11c and 11f have approximately equal small level of conservatism.

Assessment results of the failure prediction quality using Eq. (11) reported in [5] comply very well with a graphical representation of comparison of the observed and predicted cycles to failure in Fig. 11. Comparison of the total aggregate discrepancies for all considered experiments doesn't indicate the best S-N curves set, but it characterises the balance of fatigue predictions. The predictions using S-N curves {2} are unbalanced and shifted down into conservative domain. The predictions using S-N curves {1} and {3} are almost optimally balanced around the diagonal of optimal match. However, the predictions with S-N curves {3} can be considered as more accurate since all the points are closer to the diagonal with less conservative and non-conservative predictions being out of the domain for factor of 2, when compared to results obtained with S-N curves {1}. Closer look at Fig. 11 reveals that predictions with specific S-N curves {1} for SM490B steel welds have the best accuracy in long-term domain (see shaded area with $N_* > 10^6$ in Figs 11a and 11d). Predictions with generic S-N curves {2} from nCode DesignLife have the best accuracy in mid-term domain (see shaded area with $10^6 > N_* > 10^5$ in Figs 11b and 11e). Predictions with generic S-N curves {3} from nCode FE-Fatigue have the best accuracy in short-term domain (see shaded area with $N_* \sim 10^5$ in Figs 11c and 11f).

5. Conclusions

Therefore, all examined S-N curve inputs are equally good, but for different specific fatigue domains as illustrated in Fig. 12, since they all have different slopes: ~5 for S-N curves {1} for SM490B steel welds, 3 for S-N curves {2} from nCode DesignLife and ~4 for S-N curves {3} from nCode FE-Fatigue. So the most accurate fatigue predictions would be expected from a multi-slope S-N curve as suggested in Fig. 12, which is not yet available as a standard functionality for fatigue analysis of welds in nCode DesignLife. Possible candidates for the role of S-N curve with continuous range-dependent slope would be functions suggested by Bastenaire [21] or Lemaitre & Chaboche [22]

Comparing Figs 11a, 11b and 11c with Figs 11d, 11e and 11f, one can conclude that predictions using solid and shell FE-models are consistent. However, comparison of numbers N_* reported in [4, 5] indicates that predictions with solid FEs are more conservative compared to shell FEs with average differences of 20.3 %, 16.8 % and 24.9 % for each S-N curves input calculated using Eq. (11) resulting into 20.7% average difference, which is quite good. Based upon availability of ACT extension "nCode Weldline" [14] in ANSYS Workbench to facilitate the

fatigue analysis in solid formulation and reasonable conservatism of corresponding predictions, the solid FE-model fatigue analysis would be recommended as more accurate, while the shell FE-model fatigue analysis might be used for quick assessment with minimum preprocessing.

The future modelling and analysis work will address the remaining 10 fatigue tests for welded Channel-to-Channel (CC-CC) cross-beam connections (all 100 x 50 x 4CC) reported in [9]. These experiments were not included in scope of current study, since their geometry couldn't be simplified using the symmetry condition and require the consideration of whole geometry in stress and fatigue analyses. The predictions for the remaining test group are bound to prove the suggested conclusions and explanations in this study.

Acknowledgements
The authors deeply appreciate the experts of HBM - nCode for the workshops, seminars and comprehensive technical support of their leading product – nCode DesignLife. Particular gratitude is expressed to Jeffrey Mentley for an essential assistance and consultations during the course of this work.

References

[1] Moore P and Booth G 2015 *The Welding Engineer's Guide to Fracture and Fatigue* (Oxford, UK: Woodhead Publishing)
[2] Heyes P (Mar 2013) Fatigue analysis of seam welded structures using nCode DesignLife Whitepaper HBM nCode Rotherham, UK
[3] Munse W H 1978 *Fatigue Testing of Weldments (ASTM STP 648)* ed Hoeppner D W (Philadelphia, PA, USA: ASTM) pp 89–112
[4] Gorash Y, Comlekci T and MacKenzie D 2015 *Procedia Engineering* **133** 420–432
[5] Gorash Y, Comlekci T and MacKenzie D 2017 *Thin-Walled Structures* 17 p., under review
[6] Chang K H 2013 *Product Performance Evaluation with CAD/CAE* (Boston, USA: Academic Press) Chapter 4, pp 205–273
[7] Newbold P 2013 *DesignLife Theory Guide* HBM nCode Rotherham, UK Version 9 ed
[8] Mashiri F R and Zhao X L 2010 *Thin-Walled Structures* **48** 159–168
[9] Mashiri F R, Zhao X L and Tong L W 2013 *Thin-Walled Structures* **63** 27–36
[10] Fatigue Testing Division (2003, 2004, 2006, 2009, 2011) Data sheet on fatigue properties of non-load-carrying cruciform welded joints of SM490B rolled steel for welded structure: NIMS Fatigue Data Sheets No. 91, 96, 99, 108, 114 National Institute for Materials Science Tsukuba, Japan
[11] EasySteel^{TM} 2016 *The Steel Book* (Auckland, New Zealand: Fletcher Building Ltd.)
[12] Fermér M, Andréasson M and Frodin B 1998 *SAE Technical Papers No. 982311* 1–9
[13] ASME BPV Committee on Pressure Vessels 2010 *2010 ASME Boiler & Pressure Vessel Code: Section VIII Division 2 – Alternative Rules* 2010th ed (New York, USA: ASME)
[14] Mentley J 2015 nCode DesignLife Weldline ACT Extension PowerPoint Presentation, HBM - nCode Products (Southfield, MI, USA)
[15] Haibach E 2003 *FKM-Guideline: Analytical Strength Assessment of Components in Mechanical Engineering* 5th ed (FKM, Frankfurt am Main, Germany: VDMA Verlag)
[16] British Standard 2014 *Guide to fatigue design and assessment of steel products* BS 7608:2014 (London, UK: The British Standards Institution)
[17] Budynas R G and Nisbett J K 2010 *Shigley's Mechanical Engineering Design* 9th ed (New York, USA: McGraw-Hill)
[18] Australian / New Zealand Standard 2009 *Cold-formed structural steel hollow sections* AS/NZS 1163:2009 (Sydney / Wellington: Standards Australia / Standards New Zealand)
[19] AustubeMills 2013 *TS100 – angles, channels, flats* 7th ed DuraGal® Technical Specifications (Acacia Ridge, QLD, Australia: Australian Tube Mills Pty Ltd.)
[20] Zhao X L, Herion S, Packer J A, Puhtli R S, Sedlacek G, Wardenier J, Weynand K, van Wingerde A M and Yeomans N F 2001 *Design guide for circular and rectangular hollow section welded joints under fatigue loading* (Köln, Germany: TÜV-Verlag GmbH)
[21] Bastenaire F 1972 *Probabilistic Aspects of Fatigue* (*ASTM special technical publication* no STP 511) ed Heller R A (Philadelphia, USA: ASTM) chapter 1, pp 3 – 28
[22] Lemaitre J and Chaboche J-L 1994 *Mechanics of Solid Materials* (Cambridge, UK: Cambridge University Press)